Binding of the water of primary hydration to the sodium and cesium salts of deoxyribonucleic acid and potassium hyaluronate

K. B. Whitson,[1,2] A. M. Lukan,[1] R. L. Marlowe,[2] S. A. Lee,[1] L. Anthony,[1] and A. Rupprecht[3]
[1]*Department of Physics & Astronomy, University of Toledo, Toledo, Ohio 43606*
[2]*Department of Physics, Geology & Astronomy, University of Tennessee at Chattanooga, Chattanooga, Tennessee 37403*
[3]*Division of Physical Chemistry, Arrhenius Laboratory, University of Stockholm, S-106 91 Stockholm, Sweden*
(Received 29 January 1998; revised manuscript received 2 April 1998)

Differential scanning calorimetry (DSC) has been used to evaluate the average enthalpy of desorption of the water of primary hydration bound to wet-spun films of potassium hyaluronate (KHA) and CsDNA. The enthalpies were measured to be 0.24 ± 0.08 eV/H_2O molecule for KHA and 0.32 ± 0.10 eV/H_2O molecule for CsDNA. A Kissinger analysis was used to extract the net activation energy (0.61 ± 0.04 eV) for the desorption of this water from KHA by analyzing DSC data acquired at different heating rates. The average effective force constants at 295 K of this water bound to KHA (63 ± 3 μdyn/Å) and NaDNA (17 ± 4 μdyn/Å) are determined from Rayleigh scattering of Mossbauer radiation data [G. Albanese, A. Deriu, F. Cavatorta, and A. Rupprecht, Hyperfine Interact. **95**, 97 (1995)] via a harmonic approximation. [S1063-651X(98)12008-1]

PACS number(s): 87.15.By, 87.10.+e, 07.20.Fw

I. INTRODUCTION

Water of hydration is an integral part of the biologically active form of many biomolecules. Water is essential for the stabilization of the secondary and tertiary structures of nucleic acids, proteins, and glycosaminoglycans [1–5]. Hydrophobic interactions are important for proteins, since the linear polypeptide chain will fold so that most of the hydrophobic amino acids are on the interior of the protein, avoiding contact with the water molecules of solution. Hydrophobic effects also contribute to the stability of the base pairs of DNA: the hydrophobic purine and pyrimidine rings are forced to the center of the double helix [4,5]. The high dielectric function of water is responsible for significant screening of Coulombic interactions between charged sites of biomolecules. The water of hydration is usually divided into two broad categories: the strongly bound primary hydration, and the more loosely bound secondary hydration.

Given the important role that water plays in biomolecules, it is important to develop a complete understanding of the interactions between water and biomolecules. The interaction between a typical water molecule and a biomolecule is sketched in Fig. 1. The enthalpy ΔH is a measure of the energy difference between the bound and unbound states of the water molecule. The activation energy E_A is a measure of the height of the energy barrier which the water molecule must overcome for desorption. The effective force constant k is the curvature of the potential near the equilibrium separation between the water and the biopolymer. In this paper we report the measurement of the average values of these three physical parameters for water of primary hydration bound to two different biopolymers: DNA (a nucleic acid) and hyaluronic acid (HA, a glycosaminoglycan).

This paper is organized in the following manner. The remainder of Sec. I describes the essential features of the water of hydration, its effects on DNA and HA, and the Rayleigh scattering of Mossbauer radiation (RSMR) experiments of Refs. [6,7] on potassium hyaluronate (KHA) and NaDNA. The sample preparation and differential scanning calorimetry (DSC) procedures are described in Sec. II. Section III is divided into two main parts: (A) the results and analysis of the DSC experiments, and (B) the effective force constants of the bound water of primary hydration derived from the RSMR data of Refs. [6,7]. Section III A is subdivided into (1) the evaluation of the enthalpy for desorption of the water of primary hydration from HA and DNA, and (2) the evaluation of the activation energy for desorption of the water of primary hydration from HA and DNA. Section III B is subdivided into (1) the calculations of the average effective force constants using Einstein and Debye models for both HA and DNA, (2) a discussion about the structural aspects of the hydration shells in the two biopolymers, and (3) the contributions of dynamic coupling to the effective force constants. Finally, Sec. IV discusses the significance of all of our new results.

Franklin and Gosling showed that the water of hydration was important for stabilizing the DNA double helix into the *A* and *B* conformations [8]. For DNA, primary hydration extends up to a relative humidity (RH) of about 75%, corresponding to about 20 water molecules per base pair [9–11].

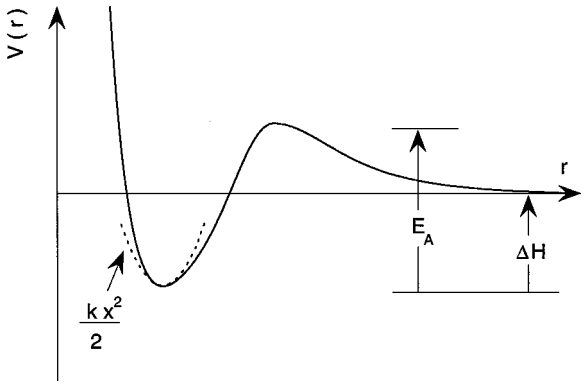

FIG. 1. Schematic representation of the interaction potential between a water molecule of primary hydration and a biomolecule as a function of their separation.

X-ray-diffraction experiments do not yield ordered patterns for DNA samples below about 50% RH (or about ten water molecules per base pair) [12], suggesting that the periodicity of the DNA molecule is disrupted as the water of primary hydration is removed. Further support for this is found in ultraviolet (UV) absorption experiments on films of DNA, which show a marked increase in the absorption at 260 nm (A_{260}) as the RH is decreased from about 65% to about 55% [13]. This absorption at 260 nm is due to electronic transitions in the four bases [14]. The dipole moments associated with these transitions are partially canceled when the bases are stacked, lowering the observed absorption. The observed increase in A_{260} as the DNA is dehydrated indicates that the bases destack as the water of primary hydration is removed. These x-ray and UV results show that double-helical structure of DNA does not exist without about ten water molecules per base pair (that is, about half of the primary hydration).

Water of hydration has also been shown to affect the conformation of HA [15,16], a polydisaccharide with a repeat unit consisting of glucuronic acid and N-acetylglucosamine. HA must have arisen very early in evolution since it is found in *streptococci*. This important biopolymer is the central organizing component of cartilage in mammals. It is also found in the intercellular matrix of connective tissues and the vitreous humor.

KHA molecules in oriented fibers or films generally adopt a fourfold single helical structure [17–20], though HA is highly polymorphic and different conformations can be induced by adjusting parameters such as water content, temperature, and applied tension [16]. X-ray-diffraction experiments on KHA have shown that either two [17,18] or four [19] water molecules per disaccharide mediate intermolecular and intramolecular interactions which stabilize the structure. The hydration of HA (the number of water molecules per disaccharide unit) has been determined by gravimetric measurements [21,22], in which the mass of HA films is measured as a function of RH. The mass of these films increases as the RH increases, since additional water molecules occupy hydration sites. These experiments have shown that the number of water molecules per HA disaccharide unit increases very rapidly as a function of RH above about 75% RH. Water content experiments on DNA reveal the same basic feature: hydration over all values of RH with a much higher number of water molecules per disaccharide above about 75% RH [9,10]. At each humidity level the number of water molecules per repeat unit (base pair for DNA and disaccharide for HA) is about twice as large for DNA as it is for HA, since each base pair of DNA has a net charge of $-2e$ while each disaccharide of HA has a net charge of $-1e$. The net charge of the biopolymers is the primary reason for their strong interaction with water, which has a very large permanent dipole moment.

The hydration process has been well studied in DNA. Falk, Poole, and Goymour [23] measured the width of an infrared (IR) absorption peak of water bound to solid DNA as a function of temperature. At room temperature this peak has a width characteristic of liquid water. (Solid ice with its long-range crystalline order has a much narrower peak.) The width of this IR peak for DNA hydrated at 76% RH remained broad down to $-150\,^{\circ}$C, indicating that the water molecules could not form an ice lattice since they are strongly bound to the DNA. These water molecules are identified as the water of primary hydration. Similar experiments on DNA hydrated at 86.5% RH revealed that a narrow component of this IR peak is observed at $-32\,^{\circ}$C. This narrow component was attributed to loosely bound water which froze into ice; these water molecules are considered to be the water of secondary hydration. The broad component of the feature was still observed for the 86.5% RH sample, indicating that the primary hydration shell is still intact under conditions of secondary hydration. Temperature-dependent Raman experiments by Tominaga *et al.* [24] and Brillouin experiments by Tao, Lindsay, and Rupprecht [25,26] verified the existence of the primary and secondary hydration shells, and measured the coupling of the water of primary hydration to the phonons of the DNA lattice. The hydration of DNA is considered to be composed of two regimes: primary hydration involving strongly bound water molecules (which is completed by about 75% RH), and secondary hydration shells involving more loosely bound water molecules (which occurs at RH's above 75%). Each of the water molecules binds to DNA with its own particular strength. It is an oversimplification to consider this hydration to involve two different binding shells, but this has proved useful in the study of DNA. X-ray diffractometry also reveals information about the binding of water to DNA. Some, but not all, of the water molecules can be located by diffractometry [27–30]; the most strongly bound water molecules (with their smaller Debye-Waller factors) are easiest to locate.

The similarity between the hydration curves of HA and DNA suggests that the hydration processes are similar in the two biopolymers. Further support for this similarity was found in the Brillouin experiments of Lee *et al.* [31]. Using a coupled-mode model to analyze their data, they found a substantial coupling between LA phonons propagating either parallel or perpendicular to the helical axis in HA films and a relaxation mode of the water of primary hydration. Both the microscopic coupling constant and the relaxation time of the water of hydration were found to be constant between 0 and 93% RH. Earlier studies on DNA revealed similar results [25,26]. The values of the coupling constant and relaxation time for water of primary hydration bound to HA and DNA are nearly equal, suggesting that the primary hydration shells are very similar for these two biomolecules. Some of the water molecules attached to HA must be very strongly bound, since they can be located by x-ray diffractometry on oriented fibers [17–19].

Increasing the water content lowers the speed of sound in both DNA [32] and HA [31,33], though the effect is particularly dramatic for HA. Brillouin scattering experiments on oriented wet-spun films of HA have shown that the sound speed decreases discontinuously by about 40% with increasing RH between 84 and 88%. X-ray diffractometry has also shown that these films undergo an order-to-disorder transition with increasing RH between 90% and 92% [33]. The fact that the drop in the sound speed and the order-to-disorder transition occurs at different water contents indicates that the phase transition occurs in two steps. The optical polarizabilities of HA also undergo significant changes above about 80% RH [22,34]. The water content of these films has also been shown to affect their UV absorption near

280 nm. As the water content is increased, the strength of the UV absorption increases. These changes are irreversible in samples which have been exposed to RH's above that corresponding to the order-to-disorder transition.

HA and DNA films have very different elastic properties at low water contents. Brillouin scattering experiments have found that the speed of sound below about 84% RH is about 40% higher in HA [31,33] than in DNA [32]. This indicates that the elastic constants of the HA films are about twice as large as in the DNA films.

Rayleigh scattering of Mossbauer radiation (RSMR) was previously performed by Albanese and co-workers [6,7] on wet-spun films of KHA and NaDNA at 75% RH. The elastic scattering intensity shows a sharp peak at about 2 Å^{-1} for samples oriented with scattering vector Q parallel to the helical direction; no peak is detected when Q is perpendicular to the helical direction. This peak is observed only when the samples are hydrated. This peak is very close in position to the first maximum of the structure factor of bulk water but is much narrower. This peak is attributed to an excitation of the ordered water molecules along the helical axis. The mean square displacement (MSD) of the water molecules in the helical direction is determined from the temperature dependence of the elastic scattering intensity of this peak. For both samples the MSD in the helical direction is found to increase approximately linearly with temperature between about 270 and 310 K. The water molecules attached to KHA are found to have a much smaller MSD than those in NaDNA, suggesting that the water molecules in the primary hydration shell of HA experience a much stiffer force than those in DNA.

In order to explore the interactions between the water of primary hydration and these biopolymers further, we have performed DSC experiments to determine the thermodynamic properties of hydrated films of KHA and CsDNA. We also performed a harmonic analysis of the RSMR data of Refs. [6,7] in order to determine the effective force constant experienced by the water of primary of hydration.

II. EXPERIMENT

NaHA was provided as a gift from Kabi-Pharmacia AB. In order to produce KHA films, the NaHA was first dialyzed three times against 1.5-M KCl. Highly crystalline thin films (about 30 μm thick) were produced by the wet-spinning technique [20,35–37], in which a solution of HA is injected via a spinneret with many small holes (about 70 μm in diameter) into a 75% ethanol solution containing 0.1-M KCl. The high concentration of ethanol causes the HA to precipitate in the form of fibrils, which are fed onto a rotating Teflon-coated drum. This drum is rotated at a speed such that the HA is pulled onto the drum at roughly 30 times the rate that the HA is extruding from the spinneret. The resulting stress produces fibers of highly oriented HA.

A Perkin-Elmer DSC-7 power-compensated differential scanning calorimeter was used to record the thermograms. This technique employs two electrically heated microfurnaces which are maintained at the same temperature in identical thermal environments. One of the furnaces is loaded with the sample of interest, while the other is left empty as a reference (control). In a typical DSC scan, the temperatures of the sample and reference furnaces are ramped from an initial to a final temperature at some specified scanning rate (usually constant), while maintaining the two furnaces at the same temperature (null balance). This is accomplished by independently controlling the Joule heat supplied to the furnaces by generally unequal electrical power, since one of the furnaces is loaded with the sample. Since the thermal environments of the furnaces are otherwise identical, the algebraic difference of these powers reflects the power required to heat the sample alone.

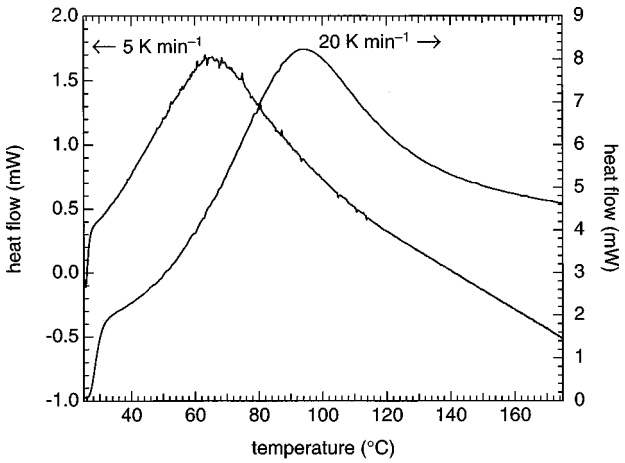

FIG. 2. Thermograms of wet-spun films of KHA, initially hydrated at 59% RH, obtained between 25 and 175 °C at scan rates of 5 and 20 K/min.

The wet-spun films of KHA were cut into pieces a few millimeters on a side, and sample masses of about 3 mg were loaded into aluminum pans of known mass. The open pans and sample were hydrated at 59% RH for at least two days by placing them over a saturated solution of sodium bromide in the bottom of a sealed glass container [38]. Each pan was covered with an aluminum lid and immediately loaded into the sample furnace of the DSC. An empty aluminum pan and lid were loaded into the reference furnace. The sample and reference furnaces were continuously purged with high-purity argon gas during all runs. Because the pans are not sealed perfectly, some water of hydration might be lost to the argon gas as the experiment begins. However, this loss is believed to be very small, since the experiment is begun soon after placing the pans in the furnaces. Runs were begun at 20 °C with temperature scanning rates of 1, 2, 5, 10, or 20 K/min. For each scanning rate, calibration runs were first performed with indium and zinc standards of known mass and purity, and their melting points were used to calibrate both the temperature and heat flow axes.

III. RESULTS AND DISCUSSION

A. DSC experiments

1. Enthalpy

Figure 2 shows two DSC thermograms for KHA obtained at scan rates of 5 and 20 K/min. A broad endothermic maximum is observed at roughly 80 °C. This broad maximum will reappear in the thermogram only if the HA sample is rehydrated, showing that this maximum is due to the desorption of the water of primary hydration. Note that the broad maximum shifts to higher temperature with increasing scan

TABLE I. Average enthalpies and activation energy barriers for desorption of the water molecules bound to KHA and CsDNA at 59% RH; and average effective force constants of the water molecules bound to KHA and NaDNA at 295 K and 75% RH.

	Enthalpy (eV/H_2O molecule)	E_A (eV)	k (μdyn/Å)
HA	0.24 ± 0.08	0.61 ± 0.04	63 ± 3
DNA	0.32 ± 0.10	0.63 ± 0.04	17 ± 4

rate. (Since the temperature axis of the instrument was calibrated at each scan rate, this is a genuine effect.) This temperature dependence of the peak position indicates that the transition is thermally activated (kinetics limited). This activation energy barrier can be determined by a Kissinger analysis [39,40] whereas the enthalpy of desorption can be determined by integrating the area under the peak. The activation barriers and enthalpies of desorption are different for each of the six water molecules attached to each HA unit. However, the DSC experiments cannot resolve the individual desorptions of these six water molecules; only a net activation energy and total enthalpy of desorption is obtainable.

The large width of the endothermic maximum introduces significant uncertainties in the enthalpy of desorption since it is difficult to determine the correct baseline. Our experiments yield an enthalpy of desorption of 0.24 ± 0.08 eV/H_2O molecule, as given in Table I. The relatively large error (33%) is primarily due to this difficulty with the background subtraction.

In our earlier report of a DSC study of wet-spun films of CsDNA [41], we only used a Kissinger analysis to determine the average activation energy for desorption. We have now evaluated the enthalpy of desorption and its uncertainties from that data. The enthalpy of desorption for DNA (at the same relative humidity) is 0.32 ± 0.10 eV/H_2O molecule [41]. The enthalpies for HA and DNA are the same to within the accuracy of the experiments, indicating that the overall binding of the water of primary hydration is very similar in these two biopolymers.

2. Activation energy

Figure 3 shows the peak temperature of the desorption as a function of scan rate. The relevant equation for determining the activation energy from the Kissinger analysis [39,40] is

$$\frac{d(\ln[\phi/T_m^2])}{d(1/T_m)} = -\frac{E_A}{k_B} \tag{1}$$

where ϕ is the scan rate, T_m is the peak temperature of the desorption, E_A is the activation energy, and k_B is Boltzmann's constant. Figure 4 is the plot of $\ln(\phi/T_m^2)$ as a function of $1/T_m$. The activation energy was obtained from the slope of a linear fit to the data and is equal to 0.61 ± 0.04 eV. A Kissinger analysis on DSC data from CsDNA gave an activation energy of 0.63 ± 0.04 eV [41]. The activation energies for these two biopolymers are very similar as were their enthalpies of desorption.

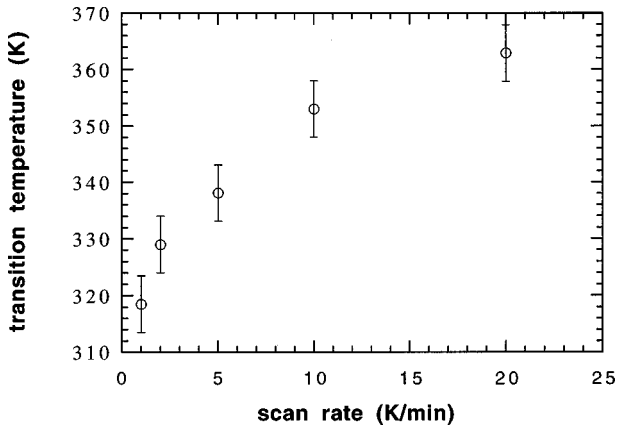

FIG. 3. Temperature of the desorption as a function of scan rate ϕ for KHA.

B. Effective force constants

1. Calculations

Biopolymers such as DNA and HA contain several different kinds of bonding: covalent bonds, hydrogen bonds, and hydrophobic and nonbonded interactions, including van der Waals and Coulomb interactions. The weak hydrogen bonding and van der Waals and hydrophobic interactions are essential for the stability of the double helix itself. These interactions are particularly difficult to describe near the ''melting'' temperature of DNA (the temperature at which the double helix denatures into two single strands). The application of the self-consistent phonon approximation (SCPA) to DNA by Prohofsky [42] represents a significant advance in the understanding of the dynamical properties of DNA, including its melting properties. In the SCPA, the definition of the simple harmonic force constant (the value of the second derivative of the potential at its minimum) is replaced by the quantum expectation value of the second derivative of the potential, calculated using the Morse potential for the hydrogen bond along with crystallographic data on the atoms' positions. As the temperature is increased, the atoms vibrate over larger distances, increasing their average separation. This weakens the interaction between these atoms and, thereby, lowers the expectation value of the second derivative of the potential. This formalism is an intuitive way

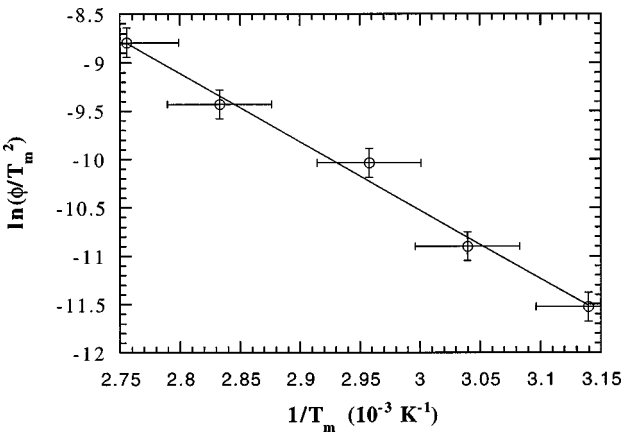

FIG. 4. Plot of $\ln(\phi/T_m^2)$ as a function of $1/T_m$ for KHA. The solid line is a linear least-squares fit to the data.

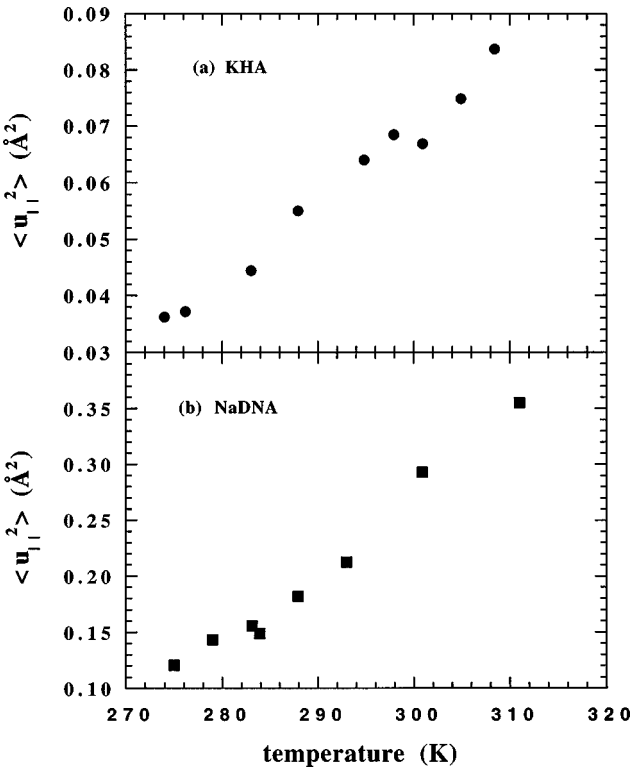

FIG. 5. Mean square displacement (MSD) of the water molecules in the direction of the helical axis for (a) KHA and (b) NaDNA as a function of temperature. The samples were hydrated to 75% RH at room temperature. The data are from Fig. 5 of Ref. [6].

to describe this system in which the second derivative varies with position. It permits the description of nonlinear problems within the harmonic approximation by allowing the effective force constants to depend on position. Normal mode calculations can be used with these effective force constants to compare them to the vibrational frequencies observed using Raman scattering and infrared absorption [43,44]. For DNA melting, such calculations show that a mode at about 85 cm^{-1} involves the stretching of the hydrogen bonds connecting the bases within a base pair. Furthermore, the frequency of this hydrogen bond stretching mode decreases as the melting temperature is approached. This softening of the mode is a consequence of the decrease of the effective force constants of these hydrogen bonds [42]. The double helix will be completely denatured when these effective force constants are zero, since there would no longer be any bonding between the two strands. Temperature-dependent Raman scattering measurements of DNA in solution by Urabe and Tominaga [45] showed that the frequency of the 85-cm^{-1} mode disappears when the DNA melts. This interpretation is supported by the calculations of Chen and Prohofsky [46].

In the spirit of the SCPA, the current system of interest (water bound to either HA or DNA) will be described by a harmonic potential in which the second derivative of the potential is a function of position (or temperature, since the MSD is temperature dependent). The effective force constants will be evaluated as a function of temperature by analyzing the $\langle u_{||}^2 \rangle$ vs T data of Refs. [6,7], where $u_{||}$ is the displacement of the water molecule in the direction parallel to the helical axis and $\langle u_{||}^2 \rangle$ is the mean square displacement in this direction. As shown in Fig. 5, the MSD is roughly four times smaller for KHA than for NaDNA, indicating that the average effective force constant for KHA is larger than for NaDNA. These data can be used to evaluate the effective force constant experienced by the water molecules of primary hydration when they are bound to the corresponding biopolymer. Though the individual water molecules in the primary hydration shell each experience somewhat different interactions with the biopolymer, we approximate the physical situation by assuming that all water molecules experience the same average interaction. As discussed in Ref. [47], the MSD for this one-dimensional case is given by

$$\langle u_{||}^2 \rangle = \frac{\hbar}{3Nm} \sum_{\mathbf{q},\lambda}^{3N} \frac{n_{\mathbf{q},\lambda} + \frac{1}{2}}{\omega_{\mathbf{q},\lambda}}, \tag{2}$$

where $\langle u_{||}^2 \rangle$ is the MSD of the water in the direction of the helical axis, N is the number of unit cells in the system, m is the mass of a water molecule, $\mathbf{q}$ and λ are the wave vectors and polarizations in the first Brillouin zone, $\omega_{\mathbf{q},\lambda}$ are the associated frequencies, $n = [\exp(\hbar \omega_{\mathbf{q},\lambda} / k_B T) - 1]^{-1}$, and k_B is Boltzmann's constant. The unit cell is a single disaccharide unit for KHA and a base pair for NaDNA, including the counterions and all of the water of hydration. At 75% RH, these unit cells contain about 11 water molecules for KHA [22] and about 20 water molecules for NaDNA [10]. The summation over $\mathbf{q}$ and λ can be transformed into an integral with respect to ω, weighted by the density of states $g(\omega)$. No experimental data currently exists for $g(\omega)$ for water bound to either biopolymer and therefore an Einstein density of states is used:

$$\langle u_{||}^2 \rangle = \frac{\hbar}{3Nm} \int d\omega \; 3N \delta(\omega - \omega_E) \frac{(n + \frac{1}{2})}{\omega}, \tag{3}$$

where ω_E is the Einstein frequency. Equation (3) reduces to

$$\langle u_{||}^2 \rangle = \frac{\hbar}{2mk_B\theta_E} \coth\left(\frac{\theta_E}{2T}\right), \tag{4}$$

where θ_E is the Einstein temperature. These θ_E are related to the effective force constants k by

$$\theta_E \equiv \frac{\hbar}{k_B} \omega_E = \frac{\hbar}{k_B} \left(\frac{k}{m}\right)^{1/2}. \tag{5}$$

Equations (4) and (5) were used to evaluate the Einstein temperature and average effective force constant at each temperature for both KHA and NaDNA from the value of $\langle u_{||}^2 \rangle$ measured in Refs. [6,7], and the results are displayed in Fig. 6. The force constant k is larger for HA than for DNA over the entire temperature range; k decreases from about 110 μdyn/Å at 274 K to about 50 μdyn/Å at 308 K for KHA, and from about 32 μdyn/Å at 275 K to about 12 μdyn/Å at 311 K for NaDNA. This indicates that the potential energy function for water bound to the biopolymer has a steeper curvature near its equilibrium position for HA than for DNA. The relative softening over the temperature range of the data is about 52% for KHA and about 62% for NaDNA, indicating that the ''stiffer'' force constant has the smaller softening (as expected). At 295 K (nominal room temperature), $k_{\mathrm{HA}} = 63 \pm 3 \mu$dyn/Å and $k_{\mathrm{DNA}} = 17 \pm 4 \; \mu$dyn/Å. The uncertain-

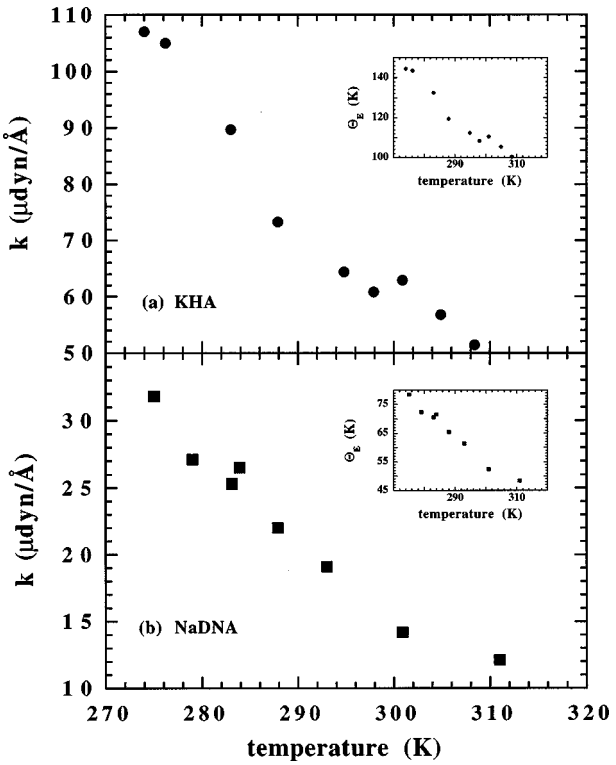

FIG. 6. Average effective force constant k for water bound to (a) KHA and (b) NaDNA as a function of temperature, as calculated by the Einstein model. The insets show the corresponding Einstein temperatures θ_E as a function of temperature. The samples were hydrated to 75% RH at room temperature.

ties are estimated from the scatter in the values of Fig. 6. The average effective force constant experienced by water molecules in the primary hydration shells of either biomolecule is weaker than the effective force constant of a typical hydrogen bond in a base pair of DNA, which is about 200 μdyn/Å [42]. However, there is a substantial difference between the two biomolecules: the average effective force constant is about 3.7 times larger for water in HA than in DNA.

We also fit the MSD data of Refs. [6,7] to a Debye model; the resulting Debye temperatures were uniformly greater than the corresponding Einstein temperatures by a factor of 1.73 ± 0.01. Of the two models (Einstein and Debye), we expect the Einstein picture to be the more appropriate one if we view the bound water molecules as being coupled primarily to the (comparatively rigid) biopolymer backbone and (relatively) weakly coupled to neighboring water molecules.

2. Structural aspects of hydration shells

Water molecules bind to DNA and HA via hydrogen bonding and other electrostatic interactions. In order to understand the microscopic origin for the observed differences in the effective force constants for HA and DNA, it is necessary to understand the binding geometry in each case. Significant progress has been made in understanding the geometry of the water tightly bound to DNA [27–29]. By examining the locations of the water molecules as determined by x-ray experiments on single crystals of 40 different oligomers, Schneider *et al.* showed that significant hydration exists in both the major and minor grooves of many types of double-helical DNA [30]. The spine of hydration in the minor groove is composed of two types of water molecules: a set of water molecules which are bound at the bottom of the groove to the nitrogen and oxygen atoms of the bases via hydrogen bonding (primary hydration), and a second set of water molecules (secondary hydration) bound to the first set of water molecules. X-ray diffractometry on HA has shown that two water molecules per repeat unit are involved in hydrogen bonding within one HA polymer and between neighboring HA polymers (via the potassium counterion) [17,18]. These bonds must be very strong since the speed of sound in HA is significantly greater than what it is observed in DNA (for directions both parallel and perpendicular to the helical axis) [33,48]. The existence of such strong bonds involving water molecules is consistent with the observation that the effective force constant is about 3.7 times greater for water bound to HA than to DNA.

3. Role of dynamic coupling

It should be noted that the two experimental techniques (calorimetry and RSMR) probe phenomena which occur on very different time scales. The DSC experiments probe long-time phenomena on time scales of tens of seconds, whereas thermally excited motions of the atoms probed by the RSMR experiments involve frequencies up to about 10 THz (on the order of the Debye frequency). As described earlier, Brillouin experiments on both DNA [25,26] and HA [31,33] have shown that LA phonons propagating in wet-spun films of these materials are coupled to a relaxational mode of the water of primary hydration. Standard coupled-mode theory [24–26,49–51] shows that such coupling can cause modifications to the frequency of the phonon depending on the relationship between that frequency and the reciprocal of the time constant τ of the relaxational mode. In the high frequency limit ($\omega \gg 1/\tau$) the coupled system is stiffened, but there is no stiffening in the low frequency limit ($\omega \ll 1/\tau$). For acoustic phonons, this stiffening results in a higher phonon velocity for the same wave vector.

There are two mechanisms by which dynamic coupling could contribute to an increase in the effective force constant of water bound to HA compared to that of water bound to DNA. First, such an enhancement would be present if the time constant of the water relaxation mode in HA is significantly larger than that in DNA. For such a case and for fixed frequency ω, dynamic coupling would stiffen the HA system if $\omega \tau_{\mathrm{HA}} \gg 1$ for the thermally excited motions, but not contribute any additional stiffening to the DNA system if $\omega \tau_{\mathrm{DNA}} \ll 1$. The second possibility is that both systems are in the high frequency limit, but the amount of stiffening in the HA system is much greater than that in the DNA system.

With regard to the first mechanism, the experiments of Refs. [25,26] and [31,33] found that the relaxation times are very similar for the two systems; about 39 ps for DNA, and about 50 ps for HA. This implies that both systems are in the high frequency regime for almost all thermally excited vibrations. Consequently, we conclude that the effective force constants of water bound to each biopolymer are both stiffened by dynamic coupling, and that the first mechanism is not relevant.

The possible importance of the second mechanism can be determined by evaluating all the parameters describing the

coupling between LA phonons with frequencies of about 10 GHz and this relaxational mode of water from the Brillouin data of Refs. [25,26] and [31,33]. For DNA, the authors of Refs. [25,26] showed that dynamic coupling makes the high frequency limit of the phonon velocity about 30% higher than the low frequency limit. The results for HA published in Refs. [31,33] can be used to determine the amount of stiffening (in the same 10-GHz frequency range) in HA by using the equation connecting the high frequency and low frequency sound speeds for the coupled-mode model [24–26,49–51]:

$$v_B^2 = v_o^2 + \left(\frac{\delta^2}{Q^2}\right)\frac{\omega_B^2\tau^2}{1+\omega_B^2\tau^2}, \tag{6}$$

where v_B is the observed velocity of the phonon with frequency ω_B and wave vector Q, v_o is the velocity the phonon would have in the zero frequency (uncoupled) limit, and δ is proportional to the coupling constant between the LA phonon and the relaxational mode of water. Such an analysis shows that dynamic coupling also stiffens these phonons by about 30%. The elastic constant in the helical direction for each sample ($C_{33}=\rho v^2$, where ρ is the density) is, therefore, stiffened by about 70%. A similar stiffening should be present in the effective force constants of both samples. Since both effective force constants are stiffened by the same amount by dynamic coupling, the second mechanism by which dynamic coupling could stiffen the effective force constants is not relevant either.

These arguments show that dynamic coupling does not play a role in explaining the observed differences between the effective force constants of water bound to HA and DNA. It is likely that the stiffness of the effective force constant of water bound to HA is related to the stiffness of ordered HA films as observed by Brillouin spectroscopy [31,33]. The fact that these films soften dramatically near the order-to-disorder transition argues that the stiffness of the system is related to the specific bonds present in the crystalline samples. The reason that these bonds are so strong is unclear at the present time.

IV. SUMMARY

The average enthalpy of desorption of the water of primary hydration is 0.24 ± 0.08 eV/H_2O molecule for KHA and 0.32 ± 0.10 eV/H_2O molecule for CsDNA. The net activation energy barrier for desorption is 0.61 ± 0.04 eV for KHA. For comparison, Marlowe *et al.* measured this net activation energy barrier to be 0.63 ± 0.04 eV for CsDNA [41]. Both these parameters are very similar in the two biopolymers. These similarities are not surprising, since these biopolymers are very similar in their constituent atoms. However, there are significant differences in the structure of their respective primary hydration shells. Spines of hydration are present in both grooves of DNA. No such structures have been observed in HA. However, water molecules are involved in both intramolecular and intermolecular binding in HA.

The effective force constants of the water bound to the biopolymer, evaluated from the measured MSD of the water molecules, are substantially different for HA and DNA: 63 ± 3 and 17 ± 4 μdyn/Å, respectively, at 295 K. The large effective force constant for HA is consistent with the fact that some of the water molecules of primary hydration are involved in the bonds between the neighboring HA polymers. The fact that the speed of sound in directions both parallel and perpendicular to the helical axis is greater in HA than in DNA indicates that the effective force constants of these intermolecular bonds in HA films are greater than the corresponding ones in DNA films. Dynamic coupling between the phonons of these biopolymers and their relaxation modes cannot account for the observed difference in these effective force constants.

ACKNOWLEDGMENTS

This work was supported in part by the NSF-REU under Grant No. PHY-9500433. K.B.W. received financial support from the University of Tennessee at Chattanooga in partial support of this work.

[1] A. J. Hopfinger, *Intermolecular Interactions and Biomolecular Organization* (Wiley, New York, 1977).

[2] I. D. Kuntz and W. Kauzmann, in *Advances in Protein Chemistry*, edited by C. B. Anfinsen, J. T. Edsall, and F. M. Richards (Academic, New York, 1974), Vol. 28, p. 239.

[3] H. Edelhoch and J. C. Osborne, in *Advances in Protein Chemistry*, Ref. [2], Vol. 30, p. 183.

[4] W. Saenger, *Principles of Nucleic Acid Structure* (Springer-Verlag, New York, 1984).

[5] J. A. McCammon and S. C. Harvey, *Dynamics of Proteins and Nucleic Acids* (Cambridge University Press, Cambridge, 1987).

[6] G. Albanese, A. Deriu, F. Cavatorta, and A. Rupprecht, Hyperfine Interact. **95**, 97 (1995).

[7] G. Albanese, F. Cavatorta, A. Deriu, and A. Rupprecht, Nuovo Cimento D **18**, 371 (1996).

[8] R. E. Franklin and R. G. Gosling, Acta Crystallogr. **6**, 673 (1953).

[9] M. Falk, K. A. Hartmann, and R. C. Lord, J. Am. Chem. Soc. **84**, 3843 (1962).

[10] N. Lavalle, S. A. Lee, and A. Rupprecht, Biopolymers **30**, 877 (1990).

[11] It should be noted the number of water molecules per base pair used in this paper is based on the assumption that there are no water molecules present when the DNA is dehydrated by drierite. Our numbers do not include the five or six water molecules per base pair which N. J. Tao, S. M. Lindsay, and A. Rupprecht [Biopolymers **28**, 1019 (1989)] assert to be present under such conditions of dehydration.

[12] S. M. Lindsay, S. A. Lee, J. W. Powell, T. Weidlich, C. Demarco, G. D. Lewen, N. J. Tao, and A. Rupprecht, Biopolymers **27**, 1015 (1988).

[13] M. Falk, K. A. Hartman, and R. C. Lord, J. Am. Chem. Soc. **85**, 391 (1963).
[14] C. R. Cantor and P. R. Schimmel, *Biophysical Chemistry Part II: Techniques for the Study of Biological Structure and Function* (Freeman, San Francisco, 1980).
[15] J. M. Guss, D. W. L. Hukins, P. J. C. Smith, W. T. Winter, S. Arnott, R. Moorhouse, and D. A. Rees, J. Mol. Biol. **95**, 359 (1975).
[16] E. D. T. Atkins and J. K. Sheehan, Science **179**, 562 (1973).
[17] A. K. Mitra, S. Arnott, and J. K. Sheehan, J. Mol. Biol. **169**, 813 (1983).
[18] A. K. Mitra, S. Raghunathan, J. K. Sheehan, and S. Arnott, J. Mol. Biol. **169**, 829 (1983).
[19] J. K. Sheehan and E. D. T. Atkins, Int. J. Biol. Macromol. **5**, 215 (1983).
[20] A. Rupprecht, Acta Chem. Scand. **33**, 779 (1979).
[21] H. Kleeberg and W. A. P. Luck, in *Glycoconjugates, Proceedings of the Fifth International Symposium*, edited by R. Schauer, P. Boer, E. Buddecke, M. F. Kramer, J. F. G. Vliegenthart, and H. Wiegandt (Thieme, Stuttgart, 1979), p. 98.
[22] S. A. Lee, M. L. VanSteenberg, N. Lavalle, A. Rupprecht, and Z. Song, Biopolymers **34**, 1543 (1994).
[23] M. Falk, A. G. Poole, and C. G. Goymour, Can. J. Chem. **48**, 1536 (1970).
[24] Y. Tominaga, M. Shida, K. Kubota, H. Urabe, Y. Nishimura, and M. Tsuboi, J. Chem. Phys. **83**, 5972 (1985).
[25] N. J. Tao, S. M. Lindsay, and A. Rupprecht, Biopolymers **26**, 171 (1987).
[26] N. J. Tao, S. M. Lindsay, and A. Rupprecht, Biopolymers **27**, 1655 (1988).
[27] M. L. Kopka, A. V. Fratini, H. R. Drew, and R. E. Dickerson, J. Mol. Biol. **163**, 129 (1983).
[28] V. N. Bartenev, Eu. I. Golovamov, K. A. Kapitonova, M. A. Mokulskii, L. I. Volkova, and I. Ya. Skuratovskii, J. Mol. Biol. **169**, 217 (1983).
[29] O. Kennard, W. B. T. Cruse, J. Nachman, T. Prange, Z. Shakked, and D. Rabinovich, J. Biomol. Struct. Dyn. **3**, 623 (1986).
[30] B. Schneider, D. M. Cohen, L. Schleifer, A. R. Srinivasan, W. K. Olson, and H. M. Berman, Biophys. J. **65**, 2291 (1993).
[31] S. A. Lee, M. R. Flowers, W. F. Oliver, A. Rupprecht, and S. M. Lindsay, Phys. Rev. E **47**, 677 (1993).
[32] S. A. Lee, S. M. Lindsay, J. W. Powell, T. Weidlich, N. J. Tao, G. D. Lewen, and A. Rupprecht, Biopolymers **26**, 1637 (1987).
[33] S. A. Lee, W. F. Oliver, A. Rupprecht, Z. Song, and S. M. Lindsay, Biopolymers **32**, 303 (1992).
[34] M. R. Flowers, R. L. Marlowe, S. A. Lee, N. Lavalle, and A. Rupprecht, Biophys. J. **63**, 323 (1992).
[35] A. Rupprecht, Acta Chem. Scand. **20**, 494 (1966).
[36] A. Rupprecht, Biotechnol. Bioeng. **12**, 93 (1970).
[37] A. Rupprecht and B. Forslind, Biochim. Biophys. Acta **204**, 304 (1970).
[38] *Handbook of Chemistry and Physics*, edited by R. C. Weast (CRC, Cleveland, 1969), Vol. 50.
[39] H. E. Kissinger, J. Res. Natl. Bur. Stand. **57**, 217 (1956).
[40] H. E. Kissinger, Anal. Chem. **29**, 1702 (1957).
[41] R. L. Marlowe, A. M. Lukan, S. A. Lee, L. Anthony, R. Chandrasekaran, and A. Rupprecht, J. Biomol. Struct. Dyn. **14**, 373 (1996).
[42] E. W. Prohofsky, *Statistical Mechanics and Stability of Macromolecules* (Cambridge University Press, Cambridge, 1995).
[43] Y. Z. Chen, A. Szabó, D. F. Schroeter, J. W. Powell, S. A. Lee, and E. W. Prohofsky, Phys. Rev. E **55**, 7414 (1997).
[44] S. A. Lee, A. Rupprecht, and Y. Z. Chen, Phys. Rev. Lett. **80**, 2241 (1998).
[45] H. Urabe and Y. Tominaga, J. Phys. Soc. Jpn. **50**, 5343 (1981).
[46] Y. Z. Chen and E. W. Prohofsky, Biopolymers **35**, 573 (1994).
[47] M. A. Krivoglaz, *Theory of X-ray and Thermal-Neutron Scattering by Real Crystals* (Plenum, New York, 1969).
[48] S. A. Lee, M. VanSteenberg, and A. Rupprecht, Carbohyd. Polym. **28**, 61 (1995).
[49] P. A. Fleury, Comments Solid State Phys. **4**, 149 (1972).
[50] A. S. Barker and J. J. Hopfield, Phys. Rev. **135**, A1732 (1964).
[51] I. J. Fritz, L. Reese, R. Brody, M. Edwards, C. M. Wilson, and H. Z. Cummins, in *Light Scattering in Solids*, edited by M. Balkanski (Flammarion, Paris, 1971), p. 415.